

Ab initio investigation of the exchange interactions in $\text{Bi}_2\text{Fe}_4\text{O}_9$: The Cairo pentagonal lattice compound

Z. V. Pchelkina^{1,2,*} and S. V. Streltsov^{1,2,†}¹*Institute of Metal Physics, S. Kovalevskoy St. 18, 620990 Ekaterinburg, Russia*²*Ural Federal University, Mira St. 19, 620002 Ekaterinburg, Russia*

(Received 2 July 2013; revised manuscript received 16 August 2013; published 28 August 2013)

We present the *ab initio* calculation of the electronic structure and magnetic properties of $\text{Bi}_2\text{Fe}_4\text{O}_9$. This compound crystallizes in the orthorhombic crystal structure with the Fe^{3+} ions forming the Cairo pentagonal lattice implying strong geometric frustration. The neutron diffraction measurements reveal nearly orthogonal magnetic configuration, which at first sight is rather unexpected since it does not minimize the total energy of the pair of magnetic ions coupled by the Heisenberg exchange interaction. Here, we calculate the electronic structure and exchange integrals of $\text{Bi}_2\text{Fe}_4\text{O}_9$ within the LSDA + U method. We obtain three different in-plane ($J_3 = 36$ K, $J_4 = 73$ K, $J_5 = 23$ K) and two interplane ($J_1 = 10$ K, $J_2 = 12$ K) exchange parameters. The derived set of exchange integrals shows that the realistic description of $\text{Bi}_2\text{Fe}_4\text{O}_9$ needs a more complicated model than the ideal Cairo pentagonal lattice with only two exchange parameters in the plane. However, if one takes into account only the two largest exchange integrals, then according to the ratio $x \equiv J_3/J_4 = 0.49 < \sqrt{2}$ [a critical parameter for the ideal Cairo pentagonal lattice, see Rousochatzakis, Läuchli, and Moessner, *Phys. Rev. B* **85**, 104415 (2012)] the ground state should be the orthogonal magnetic configuration in agreement with experiment. The microscopic origin of different exchange interactions is also discussed.

DOI: 10.1103/PhysRevB.88.054424

PACS number(s): 75.25.-j, 71.20.-b, 75.30.Et

I. INTRODUCTION

Until D. Shechtman discovered quasicrystals (the Nobel Prize in Chemistry in 2011), it was thought that it is impossible to pack atoms into a regular lattice and obey pentagonal symmetry.¹ This type of symmetry is not rare in the nature. It can be found in wild flowers and many sea dwellers as well as in a scale of a fir cone and a pineapple. The only known naturally occurring quasicrystal phase is the icosahedrite ($\text{Al}_{63}\text{Cu}_{24}\text{Fe}_{13}$) found in the Koryak Mountains in Russia. The quasicrystals reveal a new class of organization of the matter with regular but nonperiodic lattice. Such patterns have been known in the mathematics since antiquity, and medieval Islamic artists made decorative, nonrepeating tessellation (the Cairo pentagonal mosaic).

Such an exotic and rare structure is a subject of the keen interest from both experimental and theoretical point of view. As the number of bonds per elemental “brick” in the pentagonal lattice is odd, the nearest-neighbor antiferromagnetic (AFM) interactions would lead to a geometrical frustration. At present, the most studied 2D magnetic frustrated lattice is the triangular one consisting of regular polygons with equal nearest-neighbor exchange interactions. Contrary to the triangles, it is impossible to fill a plane with regular pentagons, the “bricks” of another shape are needed like in the Penrose lattice. Such a tessellation, however, can be constructed using nonregular pentagons as in the case of the Cairo pentagonal lattice.

The comprehensive analytical and numerical investigation of the antiferromagnetic Heisenberg model on the Cairo pentagonal lattice have been recently presented.² The simple pentagonal lattice studied in Ref. 2 consists of two inequivalent sites with three and four nearest neighbors (see Fig. 2 of this paper and Fig. 1 in Ref. 2). It has two types of the nonequivalent bonds, which connect the threefold sites with each other (J_{33} exchange constant) and the threefold sites

with the fourfold ones (J_{43} exchange path). Such a Cairo pentagonal lattice has the square Bravais lattice and the unit cell containing four fourfold- and two threefold-coordinated sites. The phase diagram of the AFM Heisenberg model was obtained as a function of the ratio $x \equiv J_{43}/J_{33}$ and spin S . In the classical limit (large S), three magnetic phases have been found: (1) a phase, where the spins on the neighboring sites are orthogonal to each other ($x < \sqrt{2}$), (2) the collinear 1/3-ferrimagnetic phase ($x > 2$), and (3) an intermediate mixed phase ($\sqrt{2} < x < 2$), which is a combination of (1) and (2).²

At present, there are known only two complex iron oxides that represent the physical realization of the magnetic Cairo pentagonal lattice, namely $\text{Bi}_2\text{Fe}_4\text{O}_6$ ² and $\text{Bi}_4\text{Fe}_5\text{O}_{13}\text{F}$.³ $\text{Bi}_2\text{Fe}_4\text{O}_6$ can be obtained as a byproduct in the synthesis of the multiferroic BiFeO_3 and seems to reveal multiferroic properties by itself.⁴ It is also regarded as a perspective material for the semiconductor gas sensors.⁵

$\text{Bi}_2\text{Fe}_4\text{O}_6$ crystallizes in the complex orthorhombic structure^{6,7} with the space group $Pbam$ (No. 55). It has two formula units in the unit cell and two nonequivalent iron atoms Fe_t and Fe_o occupying the tetrahedral and octahedral positions, correspondingly (see Fig. 1). The edge-sharing Fe_oO_6 octahedra form the chains along the c direction and these chains are bound by the corner-sharing Fe_tO_4 tetrahedra and Bi atoms. Fe_t occupies aforementioned threefold-coordinated sites, while Fe_o fourfold.

The magnetic measurements on a single crystal were performed in Ref. 7. At high temperature, a Curie-Weiss fitting of the magnetic susceptibility gives the paramagnetic temperature $\theta_p \approx -1670$ K and the effective magnetic moment $\mu_{\text{eff}} = 6.3(3)\mu_B$ per iron atom in agreement with value $5.9\mu_B$ corresponding to $S = 5/2$ of the Fe^{3+} ions. The long range magnetic order with $T_N = 238$ K sets in at much lower temperature indicating the presence of magnetic

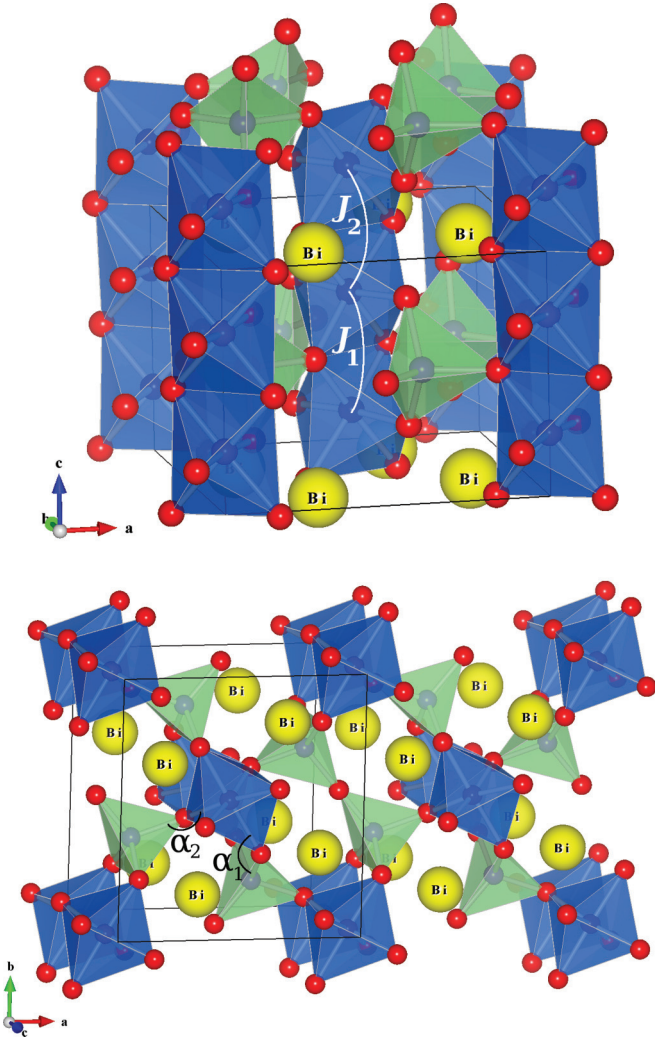


FIG. 1. (Color online) The crystal structure of $\text{Bi}_2\text{Fe}_4\text{O}_9$ along the c axis (upper panel) and in the ab plane (lower panel). There are two types of the Fe ions: Fe_o is placed in the oxygen octahedra (blue), while Fe_t is in the ligand tetrahedra (green). O and Bi are shown as red and yellow balls, respectively. J_1 and J_2 are the interplane exchange interactions. We use VESTA software⁸ for visualization.

frustrations in the system. In the unusual nearly orthogonal magnetic structure at low temperatures, the moments on all the iron atoms lying in the (a,b) plane. The Fe_o spins form four orthogonal sublattices while the Fe_t spins align antiferromagnetically with each other (see Fig. 2).

In contrast to the perfect Cairo lattice model studied in Ref. 2, the real orthorhombic crystal structure of $\text{Bi}_2\text{Fe}_4\text{O}_6$ has few distinct features. Namely, each pentagonal unit cell contains seven sites because there are two Fe_o ions in the center of the unit cell (see Fig. 1) with different coordinates along the c axis, while the ideal structure has only one. Hence, for the realistic treatment of the magnetic interactions, one needs to calculate at least five different exchange constants, which can hardly be done reliably by fitting the model solutions of the Heisenberg Hamiltonian to the magnetic susceptibility or other experimental observables. Such a fitting allows however to estimate the ratio between some of the exchange integrals.⁷

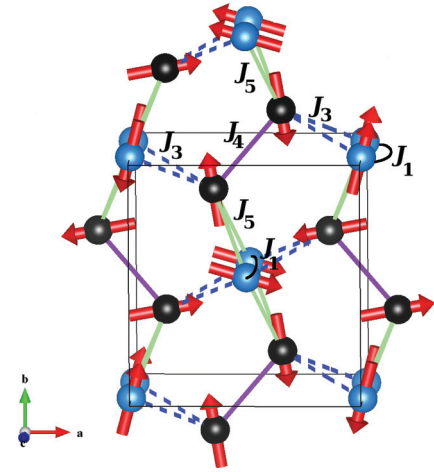


FIG. 2. (Color online) The pentagonal magnetic lattice of $\text{Bi}_2\text{Fe}_4\text{O}_9$ (ab projection) together with exchange interactions notations. The spins on each site are the same ($S = 5/2$), but the sites have different surrounding: the octahedral Fe_o ions are shown in blue, the tetrahedral Fe_t ions in black. The bonds between tetrahedral Fe_t are violet (J_4), while between octahedral Fe_o and tetrahedral Fe_t are green (J_5) and blue (J_3 , dotted line). The spin orientation represents the experimentally detected magnetic structure from Ref. 7. In the case of ideal Cairo pentagonal lattice, Fe_t ions correspond to the threefold-coordinated sites, while Fe_o correspond to the fourfold-coordinated sites. Hence, in the notation of Ref. 2, $J_4 \rightarrow J_{33}$ and $J_3 = J_5 \rightarrow J_{43}$.

In this paper, we present an *ab initio* calculation of the exchange constants in $\text{Bi}_2\text{Fe}_4\text{O}_6$, compare the result obtained with available theoretical and experimental data, show that this system cannot be considered as a realization of the perfect Cairo pentagonal lattice, and discuss the microscopic mechanisms that define the strength of different magnetic interactions.

II. CALCULATION DETAILS

We used the linearized muffin-tin orbitals method (LMTO)⁹ with the von Barth-Hedin version of the exchange correlation potential¹⁰ to calculate the electronic and magnetic properties of $\text{Bi}_2\text{Fe}_4\text{O}_9$. In order to take into account strong electronic correlations on the Fe sites, the LSDA + U approximation was applied¹¹ with the on-site Coulomb repulsion parameter $U = 4.5$ eV and the intra-atomic Hund's rule exchange $J_H = 1$ eV.^{12–14} We also checked how stable is the result with respect to the small variations of the U and J_H parameters, since the value of U may be different in different systems.¹⁵ The double counting term corresponding to the fully localized limit was used according to Ref. 11.

The Liechtenstein's exchange interaction parameter (LEIP) calculation procedure¹⁶ was used to find the intersite exchange constants for the classical Heisenberg model written as

$$H = \sum_{ij} J \vec{S}_i \vec{S}_j, \quad (1)$$

where each site in the summation is counted twice. According to this method, exchange constants J can be calculated as the second derivative of the total energy variation at small spin

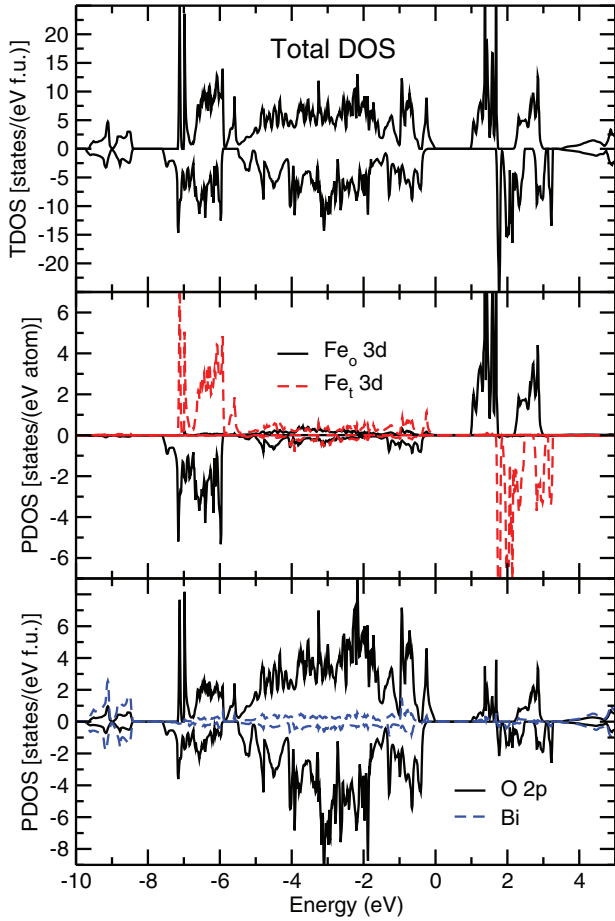


FIG. 3. (Color online) The total and partial density of states plot obtained in the LSDA + U calculation for the magnetic configuration, where all Fe_t and Fe_o are antiferromagnetically ordered. The positive (negative) values correspond to the spin up (down). The Fermi energy is in zero.

rotation. This allows to (1) calculate all J in one magnetic configuration and (2) check whether a given spin structure corresponds to the ground state or spins on some of the sites must be reversed. The later is seen from the sign of J , calculated in the LEIP method: if J is positive (i.e., the second derivative of the total energy is positive), then the total energy has a minimum for a given magnetic order, but if J is negative then one should recalculate the exchange constant for a given bond in another spin structure, since the curvature of the total energy surface and hence the value of J , in general, can be different for minima and maxima.

For the calculation of the exchange constants between the tetrahedral and octahedral Fe (J_3 and J_5 in Fig. 2), we used the magnetic configuration, where the spins on these bonds are antiferromagnetically coupled, but then the pairs of two tetrahedral Fe_t (J_4) turn out to be ferromagnetically ordered. The calculation using the LEIP method shows that the signs for J_3 and J_5 are correct (positive) for this order, but the direction of one of the spins forming J_4 path must be reversed. By checking few other magnetic configurations where spins on the Fe_t - Fe_t bond were antiferromagnetically ordered, we found that in this case, the LEIP method gives

TABLE I. The values of the exchange integrals (in K) for different U and J_H (in eV). The definition of exchange constants is shown in Fig. 2.

	J_1	J_2	J_3	J_4	J_5
$U = 4.5, J_H = 1$	10	12	36	73	23
$U = 5.5, J_H = 1$	9	9	31	64	19
$U = 4.5, J_H = 0.9$	10	12	36	72	22

positive J_4 , and its value is the same in these calculations. The same procedure was repeated for the interplane exchange coupling J_1 and J_2 . Since the signs provided by the LEIP procedure does not correspond to the usual conventions, in the following the positive (negative) exchange constants will mean antiferromagnetic (ferromagnetic) J according to the Heisenberg model presented in Eq. (1).

The crystal structure was taken from Ref. 6 and is shown in Fig. 1. The mesh of 144 k points in the Brillouin zone was used in the course of the self-consistency.

III. RESULTS

The total and partial densities of states (DOS) obtained in the LSDA + U calculation for the magnetic configuration, where all pairs of Fe_t - Fe_o are antiferromagnetically ordered are presented in Fig. 3. The DOS obtained for other magnetic structures are quite similar. The top of the valence band is mostly defined by the O $2p$ states, while the bottom of the conduction band is formed by the Fe $3d$ (spin minority) states. So that $Bi_2Fe_4O_9$ must be classified as a charge transfer insulator.¹⁷ The band gap varies from 0.97 to 1.28 eV depending on the magnetic configuration under consideration. The values of the spin moments are slightly reduced from $5 \mu_B$ expected for the Fe^{3+} ions with $S = 5/2$ due to the hybridization effects and equal 3.9–4.0 μ_B .

There are three different types of the exchange coupling in the ab plane according to our calculations [see Table I (first string) and Fig. 2]. The largest is $J_4 = 73$ K for the pair of the tetrahedral Fe_t . There are also two $J_5 = 23$ K and two $J_3 = 36$ K both between the octahedral and tetrahedral Fe ions. The main mechanism for all of them is the superexchange via oxygen ion shared by two $FeO_{6(4)}$ polyhedra. The values of these three exchange constants are different because of the quite different geometry of the Fe-O-Fe bonds and the ligand polyhedra surrounding each Fe ion.

The exchange constant between two tetrahedral Fe_t ions is the largest, because of the strong t_{2g}/t_{2g} exchange coupling. The t_{2g} orbitals are directed as much as possible to the oxygens in the tetrahedral case and three t_{2g} orbitals on each Fe_t site take part in a strong superexchange with the $2p$ orbitals of a common O, via the 180° Fe-O-Fe bond. The direct calculation using LEIP procedure shows that $J_4^{t_{2g}/t_{2g}} = 50$ K, whereas $J_4^{t_{2g}/e_g} = 16$ K and $J_4^{e_g/e_g} = 7$ K (see Table III).

If the coordinate system is chosen in a way shown in Fig. 4, it is convenient to work not with the conventional p_x , p_y , and p_z orbitals, but with $p_\sigma = (p_x + p_y + p_z)/\sqrt{3}$, $p_1 = (p_x - p_y)/\sqrt{2}$, and $p_2 = (p_x + p_y - 2p_z)/\sqrt{6}$. Then the largest p - d hopping in the tetrahedra will be between p_σ and any of the t_{2g}

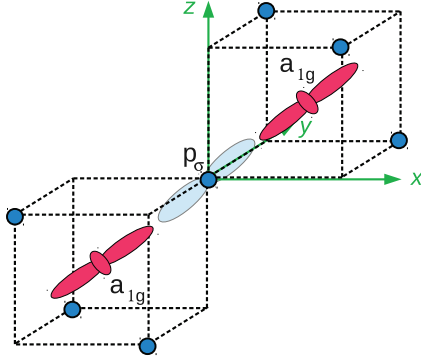


FIG. 4. (Color online) The sketch illustrating the strongest exchange coupling between a_{1g} orbitals on two tetrahedral Fe_t ions via the p_σ (light blue color) orbital, directed to the centers of tetrahedra. Oxygen ions are blue balls.

orbitals (different p - t_{2g} hopping matrix elements in the case of a regular tetrahedron are calculated in Table II with the use of the Slater-Koster parametrization¹⁸). Hence the Largest contribution to the total exchange interaction between two tetrahedral Fe_t will be the superexchange via the p_σ orbital:

$$J_{tt}^{t_{2g}/p_\sigma/t_{2g}} \sim 9 \frac{(t_{p_\sigma t_{2g}}^{\text{tet}})^2 (t_{p_\sigma t_{2g}}^{\text{tet}})^2}{U \Delta_{\text{CT}}^2}, \quad (2)$$

where Δ_{CT} is the charge transfer energy [energy of the excitation from the O $2p$ orbitals to the $3d$ shell of a transition metal ion, in our case, $\text{Fe}^{3+}(d^5)\text{O}^{2-}(2p^6) \rightarrow \text{Fe}^{2+}(d^6)\text{O}^-(2p^5)$],¹⁷ and $t_{p_\sigma t_{2g}}^{\text{tet}}$ is the hopping matrix element between p_σ and one of the t_{2g} orbitals in the FeO_4 tetrahedron. Factor 9 comes from the number of the different t_{2g} orbitals on each site. In the case of the t_{2g}/e_g exchange interaction, this prefactor will be smaller, so are the hopping integrals (there will be mostly $t_{pd\pi}$ hoppings, which are approximately two times smaller than $t_{pd\sigma}$ ¹⁹).

It is interesting that Eq. (2) can be rewritten in a more useful form if one will use a basis of the trigonal-like²⁰ orbitals also for the $3d$ states, i.e., $a_{1g} = (d_{xy} + d_{yz} + d_{zx})/\sqrt{3}$, $t_1 = (d_{yz} - d_{zx})/\sqrt{2}$, and $t_2 = (d_{yz} + d_{zx} - 2d_{xy})/\sqrt{6}$. Then, all t_{pd} hopping parameters will be zero except $t_{p_\sigma a_{1g}} = t_{pd\sigma}$, $t_{p_1 t_1} = t_{p_2 t_2} = -t_{pd\pi}/\sqrt{3}$ and there will be only two contributions to the exchange between the t_{2g} orbitals coming from the a_{1g} orbitals:

$$J_{tt}^{a_{1g}/p_\sigma/a_{1g}} \sim \frac{(t_{pd\sigma}^{\text{tet}})^4}{U \Delta_{\text{CT}}^2}, \quad (3)$$

TABLE II. The values of the p - d hopping matrix elements (t_{pd}) between the d and p orbitals [$p_\sigma = (p_x + p_y + p_z)/\sqrt{3}$, $p_1 = (p_x - p_y)/\sqrt{2}$, and $p_2 = (p_x + p_y - 2p_z)/\sqrt{6}$] in the case of the regular MeO_4 tetrahedron using the Slater-Koster parameterization,¹⁸ if the coordinate system is chosen as shown in Fig. 4.

	p_σ	p_1	p_2
d_{xy}	$\frac{1}{\sqrt{3}} t_{pd\sigma}$	0	$\frac{\sqrt{2}}{3} t_{pd\pi}$
d_{yz}	$\frac{1}{\sqrt{3}} t_{pd\sigma}$	$\frac{-1}{\sqrt{6}} t_{pd\pi}$	$\frac{-1}{3\sqrt{2}} t_{pd\pi}$
d_{zx}	$\frac{1}{\sqrt{3}} t_{pd\sigma}$	$\frac{1}{\sqrt{6}} t_{pd\pi}$	$\frac{-1}{3\sqrt{2}} t_{pd\pi}$

TABLE III. The orbital contribution (in K) for tetra-tetra exchange (J_4) and for tetra-octa exchange (J_3 and J_5) obtained within LEIP procedure with $U = 4.5$ eV and $J_H = 1$ eV.

	t_{2g}/t_{2g}	t_{2g}/e_g	e_g/e_g
J_4	50	16	7
J_5	8	8	7
J_3	13	15	8

and from the t_1 and t_2 orbitals,

$$J_{tt}^{t_1/p_\sigma/t_1} \sim \frac{2(t_{pd\pi}^{\text{tet}})^4}{9U \Delta_{\text{CT}}^2}. \quad (4)$$

Using the estimation of the interatomic matrix elements,¹⁹ it is easy to find that the ratio

$$\frac{J_{tt}^{a_{1g}/p_\sigma/a_{1g}}}{J_{tt}^{t_1/p_\sigma/t_2}} \sim 100, \quad (5)$$

so that one may think that in the case of the regular tetrahedra the t_{2g}/t_{2g} exchange with a good precision can be described solely by the superexchange between the a_{1g} orbitals via the p_σ orbital.

Since J_4 is considerably larger than other in-plane exchange couplings, it fixes the directions of the spin moments on two out of three tetrahedral Fe sites, i.e., makes spins of these Fe ions antiparallel. The exchange constants J_3 and J_5 describing coupling between the octahedral Fe_o and tetrahedral Fe_t ions are noticeably smaller than J_4 for the pair of the tetrahedral Fe_t . There are two reasons for that.

First of all, the angle of the Fe_t -O- Fe_o bond is far from 180° (the Fe_t -O- Fe_t bond angle is exactly 180°). If it was $\sim 180^\circ$ then the superexchange between the Fe_t t_{2g} and Fe_o e_g states via the O p_σ orbital would be of the order of the t_{2g}/t_{2g} superexchange in the pair of the tetrahedral Fe_t ions [the number of active orbitals (two e_g orbitals) of the octahedral Fe_o will be smaller than in the tetrahedral case (three t_{2g} orbitals), but they will be directed exactly to the oxygens]. However, this is not the case. There are two types of the tetrahedron-octahedron bonds in $\text{Bi}_2\text{Fe}_4\text{O}_9$ structure: one with the Fe_t -O- Fe_o angle $\alpha_1 \sim 120^\circ$ and another with $\alpha_2 \sim 130^\circ$ (see Fig. 1). The first one provides exchange coupling J_5 , while the second J_3 . Since $\alpha_{1,2}$ are far from both 180° and 90° , the t_{2g}/t_{2g} and t_{2g}/e_g superexchanges should be comparable. The direct calculation using LEIP formalism (see Table III) shows that for the 120° bond: $J_5^{t_{2g}/t_{2g}} = 8$ K and $J_5^{t_{2g}/e_g} = 8$ K, while for the 130° bond $J_3^{t_{2g}/t_{2g}} = 13$ K and $J_3^{t_{2g}/e_g} = 15$ K. Note, that the contribution coming from the e_g orbitals is surprisingly almost the same for these two exchange pairs: $J_5^{e_g/e_g} = 7$ K and $J_3^{e_g/e_g} = 8$ K.

The second important difference between exchanges in the Fe_t - Fe_t and Fe_t - Fe_o pairs is in the Fe-O bond distance. In the case of two tetrahedral Fe_t ions both Fe_t -O bond distances are $d(\text{Fe}_t\text{-O}) = 1.81$ Å. While for the Fe_t - Fe_o pair in the case of the bond angle $\alpha_1 = 120^\circ$ (J_5): $d(\text{Fe}_t\text{-O}) = 1.91$ Å and $d(\text{Fe}_o\text{-O}) = 2.03$ Å, while for $\alpha_2 = 130^\circ$ (J_3): $d(\text{Fe}_t\text{-O}) = 1.85$ Å and $d(\text{Fe}_o\text{-O}) = 1.97$ Å. The Fe_o -O bond distances are larger than Fe_t -O since the ionic radius of the Fe^{3+} is larger in

the octahedral coordination than in tetrahedral [$R_{\text{HS}}^{\text{IV}}(\text{Fe}^{3+}) = 0.49 \text{ \AA}$, while $R_{\text{HS}}^{\text{VI}}(\text{Fe}^{3+}) = 0.645 \text{ \AA}$].²¹

It is rather complicated to find analytically the bond and angle dependencies of all exchange constants due to the strongly distorted crystal structure and many active (magnetically) orbitals in $\text{Bi}_2\text{Fe}_4\text{O}_9$. We performed such calculations for the t_{2g}/e_g contribution to the exchange coupling between the octahedral and tetrahedral Fe ions with the 130° and 120° $\text{Fe}_t\text{-O-Fe}_o$ bonds angles. Within the fourth order of the perturbation theory and using the approximations that, as it was shown above, the $\text{Fe}_t\text{-O}$ hoppings occur only via the p_σ orbital and that they depend only on the $\text{Fe}_t\text{-O}$ bond distance, one may find that

$$J_{t_o}^{t_{2g}-e_g} \sim \sum_i \frac{(t_{p_\sigma a_{1g}}^{\text{tet}})^2 (t_{p_\sigma e_g^i}^{\text{oct}})^2}{U \Delta_{\text{CT}}^2} \sim \sum_i C (t_{p_\sigma e_g^i}^{\text{oct}})^2, \quad (6)$$

where i numerates the e_g orbitals of the octahedral Fe_o . The $t_{p_\sigma e_g^i}$ can be estimated using the Slater-Koster coefficients and atomic positions of the Fe and O ions. Then, if one takes into account only the angle dependence of the hopping matrix elements, $J_{t_o}^{t_{2g}/e_g}(130^\circ)/J_{t_o}^{t_{2g}/e_g}(120^\circ) = 1.45$. The bond length dependence can be found using the Harrison parametrization of the pd hopping integrals ($t_{pd} \sim \frac{1}{r^{3.5}}$),¹⁹ which gives $J_{t_o}^{t_{2g}/e_g}(130^\circ)/J_{t_o}^{t_{2g}/e_g}(120^\circ) = 1.22$. Taking into account both mechanisms (the angle and bond length dependence) one finds that this ratio is ~ 1.8 , which agrees reasonably with the same ratio, obtained in the LSDA + U calculation, which equals 1.9.

Calculated exchange constants are in qualitative agreement with the estimations made in Ref. 7. All exchange constants in the ab plane are antiferromagnetic and the ratio of two tetrahedral-octahedral exchange constants $J_3/J_5 \approx 1.6$ (2.15 in Ref. 7). Because of the difference between J_3 and J_5 $\text{Bi}_2\text{Fe}_4\text{O}_9$ cannot be considered as a perfect realization of the Cairo pentagonal lattice,⁷ but still the deviations are not so strong, and it makes sense to compare our situation with that of the ideal lattice. There are only two exchange constants in the perfect version of this lattice J_4 and $J_3 = J_5$. The model study of the magnetic properties of the ideal Cairo pentagonal lattice shows that its ground state corresponds to the orthogonal spin order, if $J_3/J_4 < \sqrt{2}$.² According to our calculations both $J_5/J_4 \approx 0.32$ and $J_3/J_4 \approx 0.49$ are less than $\sqrt{2}$, and hence the ground state is also expected to be described by the orthogonal spin order, exactly as it was observed experimentally.⁷

There are two types of the exchange constants that couple the octahedral Fe_o ions along the c axis. The first one, J_1 ($\text{Fe}_o\text{-Fe}_o$ bond distance 2.90 \AA), actually has to be considered as a part of the pentagonal lattice (see Fig. 2). This constant is antiferromagnetic and equals $J_1 = 10 \text{ K}$, almost a half of one of the in-plane exchanges (J_5). It brings additional (to pentagonal) frustration in the spin system, since there are four antiferromagnetic triangles linked with each pentagon, see Fig. 2. The second interplane exchange, $J_2 = 12 \text{ K}$ ($\text{Fe}_o\text{-Fe}_o$

bond distance 3.10 \AA), is antiferromagnetic as well and couples different pentagonal planes with each other.

Finally, in order to show the dependence of the exchange constants on the U and J_H parameters, we performed the calculations with $U = 5.5 \text{ eV}$ instead of 4.5 eV (with $J_H = 1 \text{ eV}$) and with $J_H = 0.9 \text{ eV}$ instead of 1 eV (with $U = 4.5 \text{ eV}$). In the first case, $J_1 = 9 \text{ K}$, $J_2 = 9 \text{ K}$, $J_3 = 31 \text{ K}$, $J_4 = 64 \text{ K}$, and $J_5 = 19 \text{ K}$, while in the second case, $J_1 = 10 \text{ K}$, $J_2 = 12 \text{ K}$, $J_3 = 36 \text{ K}$, $J_4 = 72 \text{ K}$, and $J_5 = 22 \text{ K}$ (see Table I). So that one may see that a small modification of J_H does not change the value of exchange constants, while they are decreased as U increases, since all of the J s are inversely proportional to U .

IV. CONCLUSIONS

In the present paper, we carried out the band structure calculations of $\text{Bi}_2\text{Fe}_4\text{O}_9$ and found that it must be classified as a charge transfer insulator. The investigation of the exchange constants shows that this compound cannot be considered as a perfect realization of the Cairo pentagonal lattice. First of all, there are two different exchange parameters between the tetrahedral and octahedral Fe ions. Second, the interplanar exchange coupling additionally frustrates the system. The exchange constants along the c axis are not negligibly small and exceed 50% of one of the intraplanar exchange (J_5). However, in spite of these findings, $\text{Bi}_2\text{Fe}_4\text{O}_9$ still demonstrates nearly orthogonal spin order below T_N ⁷ in accordance with the results obtained in Ref. 2, where the study of the perfect Cairo pentagonal model was performed. This is due to the fact that both exchange parameters between the tetrahedral and octahedral Fe ions (J_3 and J_5) are much smaller than the magnetic coupling between the tetrahedral Fe sites (J_4). Strong J_4 makes the spins on two out of three tetrahedral sites antiparallel, while the ratio between J_3 and J_5 defines the angles between spin moments on the rest, one tetrahedral and two octahedral Fe sites. The microscopic analysis shows that the largest contribution, $\sim 70\%$, to J_4 comes from the coupling between the t_{2g} orbitals on different sites. The deviations from the perfect Cairo pentagonal model are expected for more subtle characteristics such as, e.g., low-energy excitation spectra. However, for the full description of the magnetic properties of $\text{Bi}_2\text{Fe}_4\text{O}_9$, the calculation of the single-ion anisotropy and anisotropic exchange constants can be required.

ACKNOWLEDGMENTS

The authors thank P. Radaelli, who drew our attention on this system. This work is supported by the Russian Foundation for Basic Research via RFFI-13-02-00374, RFFI-13-02-00050, RFFI-12-02-31331, the Ministry of education and science of Russia (grants 12.740.11.0026, MK-3443.2013.2, 14.A18.21.0889) and by Samsung via GRO program. Part of the calculations were performed on the ‘‘Uran’’ cluster of the IMM UB RAS.

*pzv@ifmlrs.uran.ru

†streltsov.s@gmail.com

¹D. Shechtman, I. Blech, D. Gratias, and J. W. Cahn, *Phys. Rev. Lett.* **53**, 1951 (1984).

- ²I. Rousochatzakis, A. M. Läuchli, and R. Moessner, *Phys. Rev. B* **85**, 104415 (2012).
- ³A. M. Abakumov, D. Batuk, A. A. Tsirlin, C. Prescher, L. Dubrovinsky, D. V. Sheptyakov, W. Schnelle, J. Hadermann, and G. Van Tendeloo, *Phys. Rev. B* **87**, 024423 (2013).
- ⁴A. K. Singh, S. D. Kaushik, B. Kumar, P. K. Mishra, A. Venimadhav, V. Siruguri, and S. Patnaik, *Appl. Phys. Lett.* **92**, 132910 (2008).
- ⁵A. Poghossian, H. Abovian, P. Avakian, S. Mkrtchian, and V. Haroutunian, *Sens. Actuators, B* **4**, 545 (1991).
- ⁶A. G. Tutov, I. E. Mylnikova, N. N. Parfenova, V. A. Bokov, and S. A. Kizhaev, *Sov. Phys. Solid State* **6**, 963 (1964).
- ⁷E. Ressouche, V. Simonet, B. Canals, M. Gospodinov, and V. Skumryev, *Phys. Rev. Lett.* **103**, 267204 (2009).
- ⁸K. Momma and F. Izumi, *J. Appl. Crystallogr.* **44**, 1272 (2011).
- ⁹O. K. Andersen and O. Jepsen, *Phys. Rev. Lett.* **53**, 2571 (1984).
- ¹⁰U. von Barth and L. Hedin, *J. Phys. C* **5**, 1629 (1972).
- ¹¹V. Anisimov, F. Aryasetiawan, and A. Lichtenstein, *J. Phys.: Condens. Matter* **9**, 767 (1997).
- ¹²S. V. Streltsov and N. A. Skorikov, *Phys. Rev. B* **83**, 214407 (2011).
- ¹³A. J. Hearmon, F. Fabrizi, L. C. Chapon, R. D. Johnson, D. Prabhakaran, S. V. Streltsov, P. J. Brown, and P. G. Radaelli, *Phys. Rev. Lett.* **108**, 237201 (2012).
- ¹⁴S. V. Streltsov, J. McLeod, A. Moewes, G. J. Redhammer, and E. Z. Kurmaev, *Phys. Rev. B* **81**, 045118 (2010).
- ¹⁵V. Anisimov, D. Korotin, and S. Streltsov, *JETP Lett.* **88**, 729 (2008).
- ¹⁶A. Liechtenstein, V. Gubanov, M. Katsnelson, and V. Anisimov, *J. Magn. Magn. Mater.* **36**, 125 (1983).
- ¹⁷J. Zaanen, G. A. Sawatzky, and J. W. Allen, *Phys. Rev. Lett.* **55**, 418 (1985).
- ¹⁸J. C. Slater and G. F. Koster, *Phys. Rev.* **94**, 1498 (1954).
- ¹⁹W. Harrison, *Elementary Electronic Structure* (World Scientific, Singapore, 1999).
- ²⁰These are not true trigonal orbitals, which are defined in the chosen coordinate system as $\phi = \frac{1}{\sqrt{3}}(xy + e^{i\frac{2\pi}{3}n}xz + e^{-i\frac{2\pi}{3}n}yz)$, with $n = 0$ corresponding to a_{1g} and $n = 1, -1$ to e_g^π .
- ²¹R. D. Shannon, *Acta Crystallogr. A* **32**, 751 (1976).